

Synthesis and Characterization of Ti Complexes Using 4-*tert*-Butyl-2,6-bis(hydroxymethyl)phenol: X-ray Structures of a Confacial Biocuboctahedron with Terminal Nucleophilic Phenylmethoxide Ligands, and a Ti_4O_{16} Core Protected by Two Hydrophobic Binding Pockets

Thorsten Glaser,^{*,[a]} Ioannis Liratzis,^[a] Thomas Lügger,^[a] and Roland Fröhlich^[b]

Keywords: Tridentate ligands / O ligands / Titanium

Treatment of 4-*tert*-butyl-2,6-bis(hydroxymethyl)phenol (H_3L) with $[\text{TiO}(\text{acac})_2]$ in protic solvents at elevated temperatures leads to the formation of the dinuclear complex $(\text{Et}_4\text{N})[\text{L}_3\text{Ti}_2]$ **1**, whereas carrying out the reaction at room temperature or in aprotic solvents leads to the formation of the tetranuclear complex $(\text{Et}_4\text{N})_2[\text{L}_2(\text{HL})_4\text{Ti}_4\text{O}_2]$ **2**. Heating **2** in protic solvents leads to the formation of **1**, but **2** is stable in non-protic solvents such as THF even upon heating. Dissolving **1** in an aprotic solvent leads to the formation of **2**. The anion of **1** consists of a confacial biocuboctahedron with a $[(\text{BzO})_3\text{Ti}^{\text{IV}}(\mu_2\text{-OPh})_3\text{Ti}^{\text{IV}}(\text{OBz})_3]^-$ core. The phenylmethoxide ligands (BzO^-), and the phenolato ligands are bound to the strong Lewis acid Ti^{IV} . The bond lengths are for $\text{Ti}-\text{OBz}$ ca.

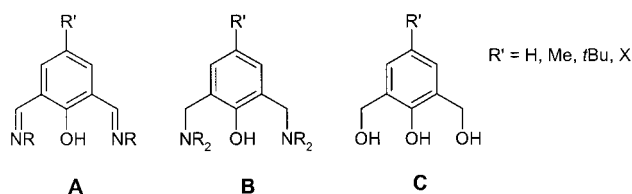
1.83 Å and for $\text{Ti}-\mu_2\text{-OPh}$ ca. 2.11 Å. Despite the highly covalent $\text{Ti}-\text{OBz}$ bond, the phenylmethoxide ligands exhibit nucleophilic character, and a tendency to bridge two Ti^{IV} ions as demonstrated by the synthesis of the tetranuclear complex **2**. The dianion in **2** consists of a Ti_4O_{16} core with two hydrophobic half-bowl shaped pockets built from three *tert*-butylbenzene units each. The hydrophobic pockets allow access to the Lewis basic $\mu_3\text{-O}^{2-}$ ligands of the Ti_4O_{16} core. In the crystal structure of $\text{2} \cdot 2\text{CH}_3\text{CN}$, two Et_4N^+ cations occupy these two binding pockets.

(© Wiley-VCH Verlag GmbH & Co. KGaA, 69451 Weinheim, Germany, 2004)

Introduction

In 1970, Robson introduced the concept of dinucleating ligands (compartmental ligands, Robson type ligands).^[1] Since then, there has been a steady increase in the number and type of such ligands synthesized in non-cyclic or macrocyclic versions. These ligands are based on the 2,6-bis(iminomethyl)phenol (**A**) and 2,6-bis(aminomethyl)phenol (**B**) backbones (Scheme 1). The synthesis of homo- and hetero-dinuclear transition metal complexes enabled detailed investigations of their magnetochemical and electrochemical properties. These studies provided important insight into the molecular and electronic structure of dinuclear metallo-proteins, and into the cooperativity of such sites in catalysis.^[2] The corresponding ligand system based on 2,6-bis(hydroxymethyl)phenol (**C**) (Scheme 1), however, has only recently been used for the synthesis of metal complexes.^[3,4] Furthermore, a search of the Cambridge Structural Database indicates that the structural coordination chemistry of phenylmethoxide ligands has, in general, not

been well explored.^[5] We are interested in dinuclear face-sharing octahedral transition metal complexes (confacial biocuboctahedra) using ligands based on **C**, because this bridging mode provides short metal-metal distances giving rise to strong electronic communications. The corresponding ligands based on **A** and **B** have already been used for the synthesis of confacial biocuboctahedra with $\text{N}_3\text{M}(\mu_2\text{-OPh})_3\text{MN}_3$ ^[6] and $\text{N}_3\text{M}(\mu_2\text{-SPh})_3\text{MN}_3$ cores.^[7] Due to their terminal facial (R_nN)₃ donor set ($n = 1$ or 2), these dinuclear complexes cannot be used as 'metal complexes as ligands' (metallo-ligands). However, confacial biocuboctahedra with a $\text{O}_3\text{M}(\mu_2\text{-OPh})_3\text{MO}_3$ core, where the terminal oxygen ligands represent monodentately coordinated alkoxide ligands, represent metallo-ligands, which can be used in a modular approach for the synthesis of larger molecules or even 1D coordination polymers.



Scheme 1

^[a] Institut für Anorganische und Analytische Chemie, Westfälische Wilhelms-Universität Münster, Wilhelm-Klemm-Straße 8, 48149 Münster, Germany
E-mail: tglaser@uni-muenster.de

^[b] Organisch-Chemisches Institut, Westfälische Wilhelms-Universität Münster, Corrensstr. 40, 48149 Münster, Germany

Herein, we report on the rational synthesis of a confacial bioctahedron with nucleophilic terminal donors. Using the ligand 4-*tert*-butyl-2,6-bis(hydroxymethyl)phenol (H_3L), the complex $(Et_4N)[L_3Ti_2]$ (**1**) with a $[(BzO)_3Ti^{IV}(\mu_2-OPh)_3-Ti^{IV}(OBz)_3]^-$ core has been synthesized and characterized. The Ti^{IV} ions are strong Lewis acids. The terminal phenylmethoxide ligands, therefore, have to donate much of their charge to the coordinated Ti^{IV} ions. However, the terminally coordinated phenylmethoxide ligands still possess sufficient nucleophilicity to bridge two Ti^{IV} ions as demonstrated by the synthesis and characterization of $(Et_4N)_2[L_2(HL)_4Ti_4O_2]$ (**2**).

Results and Discussion

Synthesis and Characterization

Treatment of H_3L with $[TiO(acac)_2]$ in a 3:2 molar ratio in the presence of a stoichiometric amount of Et_3N in refluxing MeOH yielded, after addition of excess $(Et_4N)Cl$, filtration, and slow evaporation of the solvent, yellow crystals of **1**. The IR spectrum confirmed the presence of the ligand.^[3] The absorptions at 2957, 2876, 1393, and 1363 cm^{-1} are characteristic of the *tert*-butyl groups of the ligand, and the symmetric ring stretch appears at 1479 cm^{-1} . Two strong absorptions for the stretching frequencies of the phenolic C–O bond can be observed at 1252 and 1212 cm^{-1} as well as one broad absorption of the benzylic C–O bond at 1041 cm^{-1} . Three strongly resolved absorptions at 613, 590, and 564 cm^{-1} $[v(Ti-O)]^{[8]}$ indicate the coordination of the ligand to titanium. The electrospray mass spectrum of **1** exhibits a prominent ion at a mass-to-charge ratio (m/z) of 717.6, with mass and isotope distribution patterns corresponding to $[L_3Ti_2]^-$ (calculated m/z of 717.2). The 1H and ^{13}C NMR spectra correspond to a symmetrical coordination of one kind of trianionic ligand L^{3-} . These data are all in agreement with the formulation of **1** containing the symmetric bioctahedral $[L_3Ti_2]^-$ anion.

Treatment of H_3L with $[TiO(acac)_2]$ using similar conditions used for the synthesis of **1**, but stirring the reaction solution at room temperature, yielded yellow needles of **2**. The IR spectrum clearly shows, that this change in the reaction temperature affords a complex different from **1**. Characteristic absorptions show the presence of the ligand but a broad flat absorption at 2600–3200 cm^{-1} indicates, that the ligand is not completely deprotonated. The phenolic C–O stretching region exhibits four absorptions with a different intensity pattern compared with the two absorptions observed in the spectrum of **1**, while the absorption corresponding to the stretching frequency of the benzylic C–O bond at 1040 cm^{-1} becomes smaller and broader in the spectrum of **2**. The three sharp resolved absorptions of the $v(Ti-O)$ stretches in the spectrum of **1** are replaced by several unresolved transitions in this region in the spectrum of **2**. Thus, the IR spectrum of **2** indicates a more asymmetric coordination mode of the ligand compared with in **1**, and/or the occurrence of more than one set of ligands. This is corroborated by the 1H NMR spectrum of **2**. The obser-

vation of three *tert*-butyl resonances and six different signals for the aromatic protons, demonstrates the presence of three distinguishable sets of ligand molecules in **2**. Additionally, two hydroxy proton resonances suggest, that only seven of the nine possible hydroxy groups of the three ligand molecules are deprotonated in **2**. The benzylic region shows a multitude of sharp signals indicating, that the two protons of each benzylic group are inequivalent, and that no fluxional interconversion occurs between them. Although the IR and NMR spectra of **2** show clear differences from the spectra of **1**, the electrospray mass spectrum of **2** in MeOH exhibits only a prominent ion at a mass-to-charge ratio (m/z) of 717.1 as in the spectrum of **1**, with mass and isotope distribution patterns corresponding to $[L_3Ti_2]^-$. This indicates the transformation of **2** into **1** under the conditions of the electrospray ionization (high temperature).

Single Crystal X-ray Diffraction Studies

Structure of $(NEt_4)[L_3Ti_2]$ (**1**)

The crystal structure of **1** consists of dinuclear anions $[L_3Ti_2]^-$ and well separated Et_4N^+ cations. Figure 1 shows two views of the molecular structure of the $[L_3Ti_2]^-$ anion in crystals of **1**, and the labeling scheme used. There is no crystallographic symmetry imposed on the anion. The anion consists of two titanium ions and three ligand molecules L^{3-} , which are the triply-deprotonated form of H_3L . Each ligand acts as a tridentate donor with two terminal phenylmethoxide donors (BzO^-), and one μ_2 -bridging phenolato donor (PhO^-). The two titanium ions are bridged in a face-sharing fashion by the three phenolato donors giving rise to an overall bioctahedral core. However, the coordination geometry of the titanium ions deviates severely from octahedral symmetry. Table 1 summarizes selected interatomic distances and angles of the $O_3Ti(\mu_2-O)_3TiO_3$ core. The $Ti-\mu_2-OPh$ bond lengths are in the range of 2.10–2.13 Å while the $Ti-OBz$ bond lengths are 0.3 Å shorter (1.81–1.84 Å). The $Ti1\cdots Ti2$ distance is 3.04 Å. The short $Ti-OBz$ bond lengths indicate a strong bond between the Lewis acidic Ti^{IV} ions and the Lewis basic BzO^- . The latter

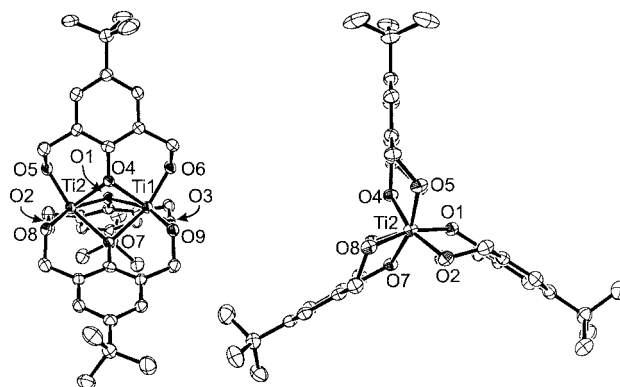


Figure 1. Two views of the molecular structure of the anion $[L_3Ti_2]^-$ in crystals of **1**

Table 1. Selected interatomic distances (Å) and angles (°) for (Et₄N)[L₃Ti₂] (**1**)

Ti1–O3 (OBz)	1.837(3)	Ti2–O2 (OBz)	1.834(2)
Ti1–O6 (OBz)	1.834(2)	Ti2–O5 (OBz)	1.835(3)
Ti1–O9 (OBz)	1.817(3)	Ti2–O8 (OBz)	1.815(2)
Ti1–O1 (μ ₂ -OPh)	2.133(2)	Ti2–O1 (μ ₂ -OPh)	2.114(2)
Ti1–O4 (μ ₂ -OPh)	2.105(2)	Ti2–O4 (μ ₂ -OPh)	2.104(2)
Ti1–O7 (μ ₂ -OPh)	2.114(2)	Ti2–O7 (μ ₂ -OPh)	2.099(2)
Ti1...Ti2	3.043(1)		
O9–Ti1–O6	97.69(11)	O2–Ti2–O5	97.75(11)
O9–Ti1–O3	95.02(11)	O8–Ti2–O7	86.02(10)
O6–Ti1–O3	94.25(11)	O2–Ti2–O7	102.54(11)
O9–Ti1–O4	107.08(11)	O5–Ti2–O7	159.14(10)
O6–Ti1–O4	85.14(10)	O8–Ti2–O4	104.36(10)
O3–Ti1–O4	157.78(11)	O2–Ti2–O4	158.86(11)
O9–Ti1–O7	85.31(10)	O5–Ti2–O4	85.67(10)
O6–Ti1–O7	158.15(11)	O7–Ti2–O4	73.66(9)
O3–Ti1–O7	107.09(10)	O8–Ti2–O1	160.48(11)
O4–Ti1–O7	73.35(9)	O2–Ti2–O1	85.17(10)
O9–Ti1–O1	158.42(10)	O5–Ti2–O1	102.49(11)
O6–Ti1–O1	103.81(10)	O7–Ti2–O1	74.75(9)
O3–Ti1–O1	85.30(10)	O4–Ti2–O1	73.75(9)
O4–Ti1–O1	73.35(9)	Ti2–O1–Ti1	91.51(9)
O7–Ti1–O1	74.05(9)	Ti2–O4–Ti1	92.60(9)
O8–Ti2–O2	95.98(11)	Ti2–O7–Ti1	92.46(9)
O8–Ti2–O5	96.68(11)		

exhibits no resonance stabilization of the negative charge compared with PhO[−].

An ideal bioctahedron would have all X–M–X angles equal to 90°, and all M–X_{br}–M (br denotes bridging ligand) angles equal to 70.53°. Distortions from this ideal geometry may be attributed to attractive or repulsive M-to-M forces.^[9] In order to compare the structure of the anion in **1** with an ideal bioctahedron, four sets of angles have to be considered: Ti1–μ₂-OPh–Ti2 (β, ideal value 70.53°), PhO–Ti–OPh (α', ideal value 90°), BzO–Ti–OBz (α'', ideal value 90°), and PhO–Ti–OBz (α''', ideal value 90°). The respective mean values of these angles in **1** are: β = 92.2°, α' = 73.7°, α'' = 96.2°, and α''' = 95.0°. The increased value of β and the decreased value of α' compared with the ideal values of 70.53° and 90°, respectively, are clear evidence of an elongation of the bioctahedron along the C₃-axis, thus indicating repulsive electrostatic interactions between the two Ti^{IV} ions. To interpret the values of α'' and α''', the steric constraints of the tridentate ligand L^{3−} must be considered. Similar constraints do not occur in confacial bioctahedra with only the monodentate ligands X, X₃M(μ₂-X)₃MX₃. The steric constraint of the phenyl ring on the methoxide CH₂O[−] units pushes the coordinated methoxide oxygen atom towards the phenyl plane of the ligand molecule (Figure 1, right). This is especially apparent with the occurrence of two different types of PhO–Ti–OBz angles (α'''). The mean value of these angles for benzylic and phenolic oxygen atoms belonging to the same ligand molecule is 85.4°, while for benzylic and phenolic oxygen atoms belonging to different ligand molecules it is 104.6°,

demonstrating the steric stress on the phenylmethoxide donors.

Structure of (Et₄N)₂[L₂(HL)₄Ti₄O₂] · 2CH₃CN (2 · 2CH₃CN)

The crystal structure of 2 · 2CH₃CN consists of tetranuclear dianions [L₂(HL)₄Ti₄O₂]^{2−}, Et₄N⁺ cations, and CH₃CN molecules. The asymmetric unit consists of one half of the dianion with the other half generated by a center of inversion. The titanium centers are in distorted octahedral coordination environments of six oxygen donors (Figure 2 and Table 2). Ti1 is coordinated by one μ₃-oxo ligand O1', one non-bridging OPh O10, one μ₂-OPh O50, two non-bridging OBz centers O19 and O51, and one μ₂-OBz O31', whereas Ti2 is coordinated by two μ₃-oxo ligands O1 and O1', one non-bridging OPh O30, one μ₂-OPh O50, one non-bridging OBz center O59, and one μ₂-OBz O31. The mean bond lengths for the different kinds of Ti–O bonds are: Ti–OBz 1.86 Å, Ti–OPh 1.90 Å, Ti–μ₃-O 1.97 Å, Ti–μ₂-OBz 2.03 Å, and Ti–μ₂-OPh 2.08 Å. The terminal phenylmethoxide donors form the shortest Ti–O bonds, while the bridging phenolato donors form the longest Ti–O bonds. It is interesting to compare these values with the corresponding values for Ti–OBz (1.83 Å) and Ti–μ₂-OPh (2.11 Å) found in **1**. The Ti–OBz bonds are slightly shorter in **1** compared with those in **2**, and the Ti–μ₂-OPh bonds are slightly longer in **1** compared with those in **2**. There are two other trends observed in the bond lengths in **2**, namely (i) the Ti–O bond length of one type of oxygen donor decreases upon going from monodentate to bridging. A ligand bridging two metal ions has to donate charge to both metal ions compared with a monodentate ligand, which only donates charge to one metal ion. Although the bridging ligand donates more overall charge (i.e. the sum of both bonds), the charge donation per bond is less compared with the bond to a monodentate ligand.^[10] This results in the observed increase in the bond lengths of the bridging ligand compared with the monodentate ligand. (ii) The Ti–O bond length of a phenylmethoxide donor is shorter than of a phenolato donor of the same coordination mode (OBz vs. OPh and μ₂-OBz vs. μ₂-OPh), which is consistent with the stronger donor ability of a phenylmethoxide ligand compared with a phenolato ligand due to the difference in resonance stabilizations of the respective anions.^[11]

The three independent ligand molecules in **2** exhibit three different coordination modes. Ligand a (O10, O11, O19) acts as a bidentate chelating ligand via O10 (OPh) and O19 (OBz), while O11 is protonated and forms an intramolecular hydrogen bond with the terminally coordinated phenylmethoxide oxygen atom O59' (2.83 Å). Ligand b (O30, O31, O39) also coordinates only in a bidentate fashion via O30 (OPh) and O31 (OBz) but the phenylmethoxide donor acts as a bridging ligand between two Ti^{IV} ions. The protonated O39 (BzOH) forms an intramolecular hydrogen bond with the terminally coordinated phenylmethoxide oxygen atom O19 (2.72 Å). The remaining ligand c (O50,

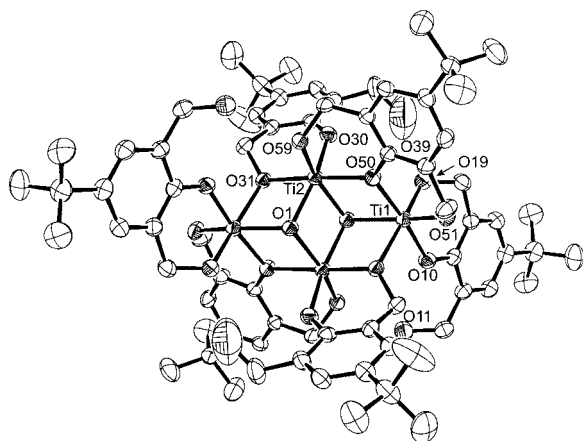


Figure 2. Molecular structure of the dianion $[L_2(HL)_4Ti_4O_2]^{2-}$ in crystals of $2 \cdot 2CH_3CN$

Table 2. Selected interatomic distances (Å) and angles (°) for $(Et_4N)_2[L_2(HL)_4Ti_4O_2] \cdot 2CH_3CN$ ($2 \cdot 2CH_3CN$)

Symmetry transformations used to generate equivalent atoms: ' $-x + 1, -y + 1, -z + 1$

Ti1–O1' (μ_3 -O)	1.967(2)	Ti2–O30 (OPh)	1.903(2)
Ti1–O10 (OPh)	1.902(2)	Ti2–O31 (μ_2 -OBz)	1.978(2)
Ti1–O19 (OBz)	1.852(3)	Ti2–O50 (μ_2 -OPh)	2.049(2)
Ti1–O50 (μ_2 -OPh)	2.102(2)	Ti2–O59 (OBz)	1.874(2)
Ti1–O51 (OBz)	1.844(2)	Ti1...Ti2	3.2083(8)
Ti1–O31' (μ_2 -OBz)	2.080(2)	Ti1...Ti2'	3.1226(9)
Ti2–O1 (μ_3 -O)	1.949(2)	Ti2...Ti2'	3.0297(11)
Ti2–O1' (μ_3 -O)	1.999(2)		
O51–Ti1–O19	98.27(12)	O59–Ti2–O31	99.72(10)
O51–Ti1–O10	95.82(11)	O30–Ti2–O31	85.61(10)
O19–Ti1–O10	88.97(11)	O1–Ti2–O31	77.58(9)
O51–Ti1–O1'	155.97(11)	O59–Ti2–O1'	158.50(10)
O19–Ti1–O1'	97.72(10)	O30–Ti2–O1'	95.59(11)
O10–Ti1–O1'	102.29(10)	O1–Ti2–O1'	79.76(10)
O51–Ti1–O31'	91.42(11)	O31–Ti2–O1'	100.36(9)
O19–Ti1–O31'	169.01(10)	O59–Ti2–O50	84.47(9)
O10–Ti1–O31'	84.87(10)	O30–Ti2–O50	94.51(10)
O1'–Ti1–O31'	74.81(9)	O1–Ti2–O50	101.67(10)
O51–Ti1–O50	85.36(10)	O31–Ti2–O50	175.80(9)
O19–Ti1–O50	97.34(10)	O1'–Ti2–O50	75.44(9)
O10–Ti1–O50	173.35(10)	Ti2–O1–Ti1'	105.75(11)
O1'–Ti1–O50	74.89(9)	Ti2–O1–Ti2'	100.24(10)
O31'–Ti1–O50	88.56(9)	Ti1'–O1–Ti2'	108.00(10)
O59–Ti2–O30	93.53(11)	Ti2–O31–Ti1'	100.60(10)
O59–Ti2–O1	97.19(10)	Ti2–O50–Ti1	101.23(9)
O30–Ti2–O1	161.34(10)		

O51, O59) exhibits the same tridentate coordination mode as the ligands in **1**.

The structure of **2** may be regarded as consisting of a Ti_4O_{16} core enclosed by an organic shell [Figure 3 (a)]. The oxygen atoms are situated above and below a plane comprised of the four titanium ions. Two half-bowls each formed by three *tert*-butylbenzene moieties are positioned above and below this Ti_4 -plane, respectively. Figure 3 (b) demonstrates that the hydrophobic half-bowl allows access to the μ_3 -oxo ligand. Thus, two hydrophobic binding pock-

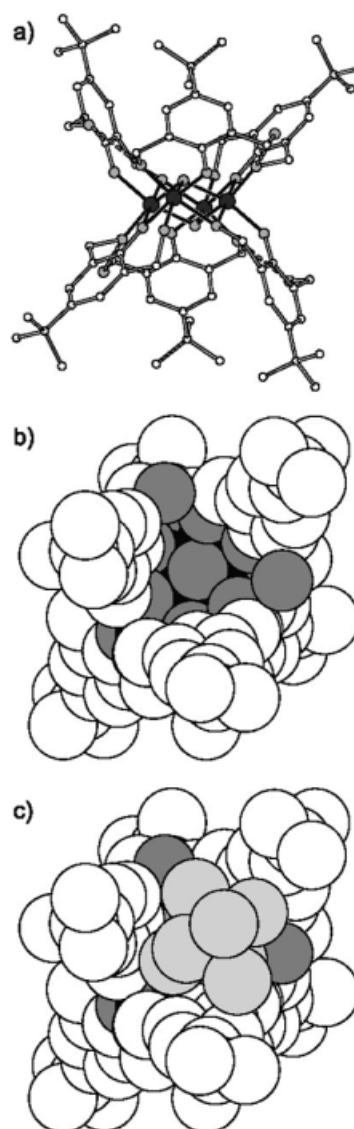


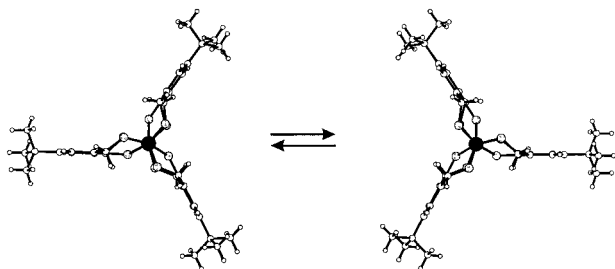
Figure 3. a) Sketch of the molecular structure of the dianion $[L_2(HL)_4Ti_4O_2]^{2-} \cdot 2 \cdot 2CH_3CN$ illustrating the Ti_4O_{16} core and the two hydrophobic half-bowls each formed by three *tert*-butylbenzene units; b) Space-filling model of this structure [rotated by 90° relative to the view in a)] illustrating the hydrophobic pocket, which allows direct access to the μ_3 -oxo oxygen atom of the Ti_4O_{16} core; c) Space-filling model of the dianion, and one Et_4N^+ cation placed in the hydrophobic pockets of the dianion

ets for Lewis bases are provided by **2**. In the crystal structure of $2 \cdot 2CH_3CN$, the two hydrophobic pockets of each dianion are occupied by the two Et_4N^+ cations [Figure 3 (c)]. The Ti_4O_{16} core found in the dianion of **2** represents a relatively common structural motif in Ti–oxygen chemistry since it has been observed in several complexes constructed from varying kinds of alkoxide ligands from monodentate to tridentate.^[4,12] These compounds can be used as molecular precursors for metal oxides in sol-gel chemistry or for thin-film preparation.

Solution Properties

The monoanion of **1** has an idealized C_{3h} symmetry in the solid state. If this symmetry were to be retained in solu-

tion, two sets of signals would be expected for the benzylic protons in the ^1H NMR spectrum. However, the ^1H NMR spectrum of **1** in $[\text{D}_6]\text{DMSO}$ exhibits only one broad resonance for the benzylic protons at $\delta = 5.17$ ppm. This indicates that a dynamic equilibrium exists between two forms with different orientations of the methoxide groups relative to the phenolic plane (Scheme 2). On the other hand, the ^1H NMR spectrum of **2** in $[\text{D}_8]\text{THF}$ solution displays all signals predicted for the three different ligand molecules observed in the solid-state structure. This means, that the conformation of the tetranuclear dianion is fixed, which could be a consequence of the four intramolecular hydrogen bonds.



Scheme 2

The UV/Vis absorption spectra of acetonitrile solutions of H_3L , **1**, and **2** are shown in Figure 4. The protonated ligand exhibits absorptions at 309 nm (sh, $\approx 120 \text{ M}^{-1} \text{ cm}^{-1}$) and 282 nm ($2320 \text{ M}^{-1} \text{ cm}^{-1}$). The spectrum of complex **1** exhibits absorption intensity, which starts to increase starting at ≈ 400 nm with no resolved transitions but shoulders at ≈ 288 , 246, and 222 nm. The absorption of the tetranuclear complex **2** starts to increase at ≈ 450 nm with maxima at 333 nm ($22200 \text{ M}^{-1} \text{ cm}^{-1}$), 296 nm ($21600 \text{ M}^{-1} \text{ cm}^{-1}$), and 290 nm ($21600 \text{ M}^{-1} \text{ cm}^{-1}$). The strong low-energy absorptions in the spectra of **1** and **2** are oxygen-to-titanium charge transfer in origin. The main conclusion is that **1** and **2** are clearly distinguishable by their absorption spectra. The spectrum of **2** measured in THF is identical to that measured in CH_3CN .

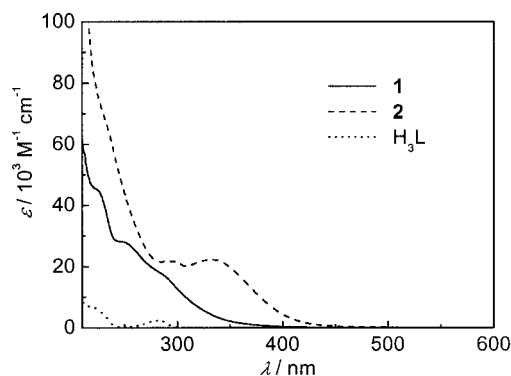
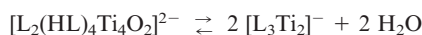


Figure 4. UV-Vis absorption spectra of acetonitrile solutions of H_3L , **1**, and **2**

Heating **2** in protic solvents leads to the formation of **1**, an essential fact for the controlled synthesis of **1** and **2**, respectively. The reaction between the ligand and $[\text{TiO}(\text{acac})_2]$ in alcoholic solution at room temperature results in the formation of **2**, whereas **1** is formed by heating the reaction mixture to reflux. This is corroborated with the ESI mass spectrum of a methanolic solution of **2** which, due to heating of the solution in the ESI process, exhibits only the signal corresponding to the anion of **1**. On the other hand, in non-protic solvents **2** is stable even upon heating. Storing the sealed NMR tube of the $[\text{D}_8]\text{THF}$ solution of **2** at 70°C overnight does not affect the ^1H NMR spectrum. Additionally, **1** can be converted back to **2**. Dissolving **1** in a $\text{CH}_3\text{CN}/\text{MeOH}$ mixture (10:1) leads to the deposition of yellow crystals, which were shown to be pure **2** by FTIR spectroscopy and single-crystal X-ray diffraction. These observations are in agreement with the following equilibrium:



The cleavage of the titanium–oxo bond of the former titanyl unit requires some activation energy, and a protic solvent is needed for the formation of water. The dinuclear $[\text{L}_3\text{Ti}_2]^-$ complex seems to be more stable in protic solvents whereas the tetranuclear $[\text{L}_2(\text{HL})_4\text{Ti}_4\text{O}_2]^{2-}$ complex seems to be more stable in aprotic solvents. The latter might indicate that the two Et_4N^+ cations remain in the hydrophobic binding pockets to give an overall neutrally charged ion triple.

Conclusions

We have shown by the synthesis of complex **1**, that 2,6-bis(hydroxymethyl)-4-*tert*-butylphenol is capable of forming a confacial biotetrahedron with a $[(\text{BzO})_3\text{Ti}^{\text{IV}}(\mu_2\text{-OPh})_3\text{Ti}^{\text{IV}}(\text{OBz})_3]^-$ core exhibiting a short $\text{Ti}\cdots\text{Ti}$ distance of $\approx 3.0 \text{ \AA}$. The coordination of the terminal phenylmethoxide donors to the strong Lewis acid Ti^{IV} still leaves some nucleophilicity at the oxygen atoms. This has been demonstrated with the synthesis of complex **2**, which exhibits μ_2 -bridging phenylmethoxide ligands. Work is in progress to prepare coordination polymers using the anion of **1** as a building block.

The tetranuclear dianion in **2** consists of a Ti_4O_{16} core protected by two hydrophobic pockets, which allow access to the μ_3 -oxo ligand of the Ti_4O_{16} core. TiO_2 is known as a heterogeneous photocatalyst, e.g. for the oxidation of ethanol.^[13] Studies on the binding of ethanol to **2** are in progress to evaluate the potential of **2** as a homogeneous photocatalyst utilizing the strong LMCT absorption band at 333 nm.

Experimental Section

General Methods and Materials: Infrared spectra ($400\text{--}4000 \text{ cm}^{-1}$) of solid samples were recorded in KBr disks using a Bruker Vector

22 spectrometer. UV/Vis/NIR-absorption spectra of solutions were measured on a Varian Cary 50 spectrophotometer in the range of 190–1100 nm at ambient temperature. ESI mass spectra were recorded on a Micromass Quattro LC mass spectrometer. ^1H and ^{13}C NMR spectra were obtained on a Bruker AC200 or on a Bruker ARX300 spectrometer using the solvent resonances as an internal standard in each case. The ligand H_3L was synthesized according to a published procedure.^[3]

(Et_4N)[L_3Ti_2] (1): To a stirred solution of H_3L (500 mg, 2.38 mmol) and $[\text{TiO}(\text{acac})_2]$ (415 mg, 1.59 mmol) in MeOH (40 mL) was added Et_3N (1.00 mL, 7.13 mmol). The yellow solution was heated to reflux for 5 h. Addition of $(\text{Et}_4\text{N})\text{Cl}$ (4.0 g), filtration, and slow evaporation of the solvent yielded yellow crystals of $(\text{Et}_4\text{N})[\text{L}_3\text{Ti}_2]$ (350 mg, 52%). $\text{C}_{44}\text{H}_{65}\text{NO}_9\text{Ti}_2$ (847.77): calcd. C 62.34, H 7.73, N 1.65; found C 62.01, H 7.58, N 1.51. MS (ESI in MeOH/ CH_3CN solution, negative ion mode): $m/z = 749.6$ $\{[\text{L}_3\text{Ti}_2]\text{MeOH}\}^-$, 717.6 $[\text{L}_3\text{Ti}_2]^-$. ^1H NMR (300 MHz, $[\text{D}_6]\text{DMSO}$, 25 °C): $\delta = 1.13$ (t, $J_{\text{H,H}} = 7.4$, $J_{\text{H-N}} = 1.8$ Hz, 12 H, NCH_2CH_3), 1.21 (s, 27 H, *tert*-butyl CH_3), 3.17 (q, 8 H, NCH_2CH_3), 5.17 (s, 12 H, br, benz. CH), 6.94 (s, 6 H, arom. CH). ^{13}C NMR (75 MHz, $[\text{D}_6]\text{DMSO}$, 25 °C): $\delta = 7.0$ (NCH_2CH_3), 31.3 ($\text{C}(\text{CH}_3)_3$), 33.4 ($\text{C}(\text{CH}_3)_3$), 51.4 (t, $J_{\text{C-N}} = 2.6$ Hz, NCH_2CH_3), 71.0 (benz. CH_2), 122.2 ($\text{C}_{\text{Ar-3}}$), 127.8 ($\text{C}_{\text{Ar-4}}$), 139.8 ($\text{C}_{\text{Ar-2}}$), 154.5 ($\text{C}_{\text{Ar-1}}$). IR: $\tilde{\nu} = 2957$ s, 2876 m, 2827 m, 1608 w, 1479 vs, 1451 s, 1393 w, 1363 w, 1252 vs, 1212 vs, 1041 vs/br, 871 w, 832 m, 765 m, 755 m, 668 m, 613 vs, 590 vs, 564 s cm^{-1} .

(Et_4N) $_2$ [$\text{L}_2(\text{HL})_4\text{Ti}_4\text{O}_2$] $\cdot 2\text{EtOH} \cdot 2\text{H}_2\text{O}$ ($2\cdot 2\text{EtOH} \cdot 2\text{H}_2\text{O}$): To a stirred solution of H_3L (500 mg, 2.38 mmol) and $[\text{TiO}(\text{acac})_2]$ (415 mg, 1.59 mmol) in EtOH (45 mL) was added Et_3N (1.00 mL, 7.13 mmol). The yellow solution was stirred at room temperature for 5 h. Addition of $(\text{Et}_4\text{N})\text{Cl}$ (4.0 g), filtration, and slow evaporation of the solvent yielded yellow needles of $(\text{Et}_4\text{N})_2[\text{L}_2(\text{HL})_4\text{Ti}_4\text{O}_2] \cdot 2\text{EtOH} \cdot 2\text{H}_2\text{O}$ (300 mg, 42%). $\text{C}_{88}\text{H}_{142}\text{N}_2\text{O}_{24}\text{Ti}_4$ (1803.61): calcd. C 58.60, H 7.94, N 1.55; found C 58.71, H 7.71, N 1.58. ^1H NMR (200 MHz, $[\text{D}_8]\text{THF}$, 25 °C): $\delta = 0.35$ (m, 24 H, NCH_2CH_3), 1.19 (s, 27 H, *tert*-butyl CH_3), 1.23 (s, 27 H, *tert*-butyl CH_3), 1.25 (s, 27 H, *tert*-butyl CH_3), 3.88 (q, 16 H, NCH_2CH_3), 4.5–6.0 (m, 24 H, benz. CH), 6.8–7.2 (6s, 12 H, arom. CH), 7.87 (s, 2 H, BzOH), 8.42 (s, 2 H, BzOH). IR: $\tilde{\nu} = 2953$ s, 2904 m, 2866 m, 1606 w, 1479 vs, 1393 w, 1364 w, 1305 w, 1275 s, 1262 s, 1218

vs, 1040 m/br, 1005 w, 877 w, 839 s, 768 m, 540–630 br cm^{-1} . X-ray quality crystals of $2\cdot 2\text{CH}_3\text{CN}$ were grown from MeOH/ CH_3CN , 1:5.

X-ray Crystallographic Data Collection and Refinement of the Structures: A summary of the crystal data, data collection, and refinements of the both structures is given in Table 3. Data sets were collected with Bruker AXS APEX and Nonius KappaCCD diffractometers, equipped with rotating anode generators. Programs used: data collection – SMART^[14] and COLLECT^[15] data reduction – SAINT^[14] and Denzo-SMN^[16] absorption correction – SADABS^[14] and SORTAV^[17] structure solution – SHELXS-97^[18] structure refinement – SHELXL-97^[19] CCDC-220429 (1) and -220430 ($2\cdot 2\text{CH}_3\text{CN}$) contain the supplementary crystallographic data for this paper. These data can be obtained free of charge at www.ccdc.cam.ac.uk/conts/retrieving.html [or from the Cambridge Crystallographic Data Center, 12 Union Road, Cambridge CB2 1EZ, UK; Fax: (internat.) +44-1223-336-033; E-mail: deposit@ccdc.cam.ac.uk].

Acknowledgments

T. G. gratefully acknowledges generous support from Prof. F. E. Hahn. This work was supported by the Fonds der Chemischen Industrie, the Bundesministerium für Bildung und Forschung, the Dr. Otto Röhm Gedächtnisstiftung, and the Deutsche Forschungsgemeinschaft (Priority Program “Molecular Magnetism”). The skilful technical assistance of Mrs. T. Pape is gratefully acknowledged.

Table 3. Crystal data and structure refinement for 1 and $2\cdot 2\text{CH}_3\text{CN}$

	1	$2\cdot 2\text{CH}_3\text{CN}$
Chemical formula	$\text{C}_{44}\text{H}_{65}\text{NO}_9\text{Ti}_2$	$\text{C}_{92}\text{H}_{140}\text{N}_4\text{O}_{20}\text{Ti}_4$
Molecular mass	847.77	1813.68
Crystal system	monoclinic	monoclinic
Space group	$C2/c$ (No. 15)	$P2_1/c$ (No. 14)
$a / \text{\AA}$	43.409(7)	14.493(1)
$b / \text{\AA}$	9.632(2)	19.454(1)
$c / \text{\AA}$	26.008(4)	16.956(1)
$\beta / ^\circ$	126.122(4)	97.06(1)
$V / \text{\AA}^3$	8784(2)	4744.4(5)
Z	8	2
T / K	153	198
μ / cm^{-1}	4.17	3.93
No. data collected	17743	29946
No. unique data	5645	11286
R_{int}	0.054	0.044
Final $R(F)$ obsd.	0.045	0.072
Final $R(F^2)$ all	0.125	0.224

- [1] [1a] R. Robson, *Inorg. Nucl. Chem. Lett.* **1970**, 6, 125–128. [1b] R. Robson, *Aust. J. Chem.* **1970**, 23, 2217–2224. [1c] N. H. Pilkington, R. Robson, *Aust. J. Chem.* **1970**, 23, 2225–2236.
- [2] [2a] F. L. Urbach in *Metal Ions in Biological Systems* (Ed. H. Sigel), Marcel Dekker, New York, **1981**, vol. 12, p. 73–115. [2b] C. L. Spiro, S. L. Lambert, T. J. Smith, E. N. Duesler, R. R. Gagne, D. N. Hendrickson, *Inorg. Chem.* **1981**, 20, 1229–1237. [2c] D. E. Fenton, H. Okawa, *Chem. Ber./Recueil* **1997**, 130, 433–442. [2d] S. Albedyhl, M. T. Averbuch-Pouchot, C. Belle, B. Krebs, J. L. Pierre, E. Saint-Aman, S. Torelli, *Eur. J. Inorg. Chem.* **2001**, 1457–1464. [2e] C. Sudbrake, H. Vahrenkamp, *Eur. J. Inorg. Chem.* **2001**, 751–754. [2f] S. Brooker, P. D. Croucher, T. C. Davidson, G. S. Dunbar, A. James McQuillan, G. B. Jameson, *Chem. Commun.* **1998**, 2131–2132. [2g] I. A. Koval, D. Pursche, A. F. Stassen, P. Gamez, B. Krebs, J. Reedijk, *Eur. J. Inorg. Chem.* **2003**, 1669–1674. [2h] G. Steinfeld, V. Lozan, B. Kersting, *Angew. Chem.* **2003**, 115, 2363–2365; *Angew. Chem. Int. Ed.* **2003**, 42, 2261–2263.
- [3] T. Glaser, T. Lügger, *Inorg. Chim. Acta* **2002**, 337, 103–112.
- [4] A. Rammel, F. Brisach, J. Henry, *J. Am. Chem. Soc.* **2001**, 123, 5612–5613.
- [5] [5a] B. Müller, A. Schneider, M. Tesmer, H. Vahrenkamp, *Inorg. Chem.* **1999**, 38, 1900–1907. [5b] R. Walz, K. Weis, M. Ruf, H. Vahrenkamp, *Chem. Ber./Recueil* **1997**, 130, 975–980.
- [6] [6a] C. J. Fahrni, A. Pfaltz, M. Neuburger, M. Zehnder, *Helv. Chim. Acta* **1998**, 81, 507–524. [6b] P. Chakraborty, S. K. Chandra, *Polyhedron* **1994**, 13, 683–687. [6c] Q. Zeng, S. Gou, L. He, Y. Gong, X. You, *Inorg. Chim. Acta* **1999**, 287, 14–20. [6d] M. D. Timken, W. A. Marritt, D. N. Hendrickson, R. A. Gagne, E. Sinn, *Inorg. Chem.* **1985**, 24, 4202–4208.
- [7] [7a] B. Kersting, D. Siebert, *Inorg. Chem.* **1998**, 37, 3820–3828. [7b] B. Kersting, D. Siebert, D. Volkmer, M. J. Kolm, C. Janiak, *Inorg. Chem.* **1999**, 38, 3871–3882. [7c] G. Steinfeld, B. Kersting, *Chem. Commun.* **2000**, 205–206. [7d] B. Kersting, G. Siedle, *Z. Naturforsch., Teil B* **2000**, 55, 1179–1187.

- [8] P. Jeske, G. Haselhorst, T. Weyhermüller, K. Wieghardt, B. Nuber, *Inorg. Chem.* **1994**, 33, 2462–2471.
- [9] [9a] F. A. Cotton, D. A. Ucko, *Inorg. Chim. Acta* **1972**, 6, 161–172. [9b] R. H. Summerville, R. Hoffman, *J. Am. Chem. Soc.* **1979**, 101, 3821–3831.
- [10] [10a] T. Glaser, K. Rose, S. E. Shadle, B. Hedman, K. O. Hodgson, E. I. Solomon, *J. Am. Chem. Soc.* **2001**, 123, 442–454. [10b] T. Glaser, B. Hedman, K. O. Hodgson, E. I. Solomon, *Acc. Chem. Res.* **2000**, 33, 859–868.
- [11] K. Rose, S. E. Shadle, T. Glaser, S. de Vries, A. Cherepanov, G. W. Canters, B. Hedman, K. O. Hodgson, E. I. Solomon, *J. Am. Chem. Soc.* **1999**, 121, 2353–2363.
- [12] [12a] S. Weymann-Schildknecht, M. Henry, *J. Chem. Soc., Dalton Trans.* **2001**, 2425–2428. [12b] J. A. Ibers, *Nature* **1963**, 197, 686–687. [12c] D. A. Wright, D. A. Williams, *Acta Crystallogr., Sect. B* **1968**, 24, 1107–1114. [12d] T. J. Boyle, R. W. Schwartz, R. J. Doedens, J. W. Ziller, *Inorg. Chem.* **1995**, 34, 1110–1120. [12e] A. I. Yanovskii, F. M. Dolgushin, M. I. Yanovskaya, N. M. Kotova, Y. T. Struchkov, N. Y. Turova, *Zh. Neorg. Khim.* **1997**, 42, 450–453.
- [13] [13a] M. A. Fox, M. T. Dulay, *Chem. Rev.* **1993**, 93, 341–357. [13b] D. S. Muggli, J. L. Falconer, *J. Catal.* **1998**, 175, 213–219. [13c] R. Wittenberg, M. A. Pradera, J. A. Navio, *Langmuir* **1997**, 13, 2373–2379. [13d] L.-F. Liao, W.-C. Wu, C.-Y. Chen, J.-L. Lin, *J. Phys. Chem. B* **2001**, 105, 7678–7685.
- [14] Bruker AXS, **2000**.
- [15] Nonius B. V., **1998**.
- [16] Z. Otwinowski, W. Minor, *Methods Enzymol.* **1997**, 276, 307–326.
- [17] [17a] R. H. Blessing, *Acta Crystallogr., Sect. A* **1995**, 51, 33–37. [17b] R. H. Blessing, *J. Appl. Cryst.* **1997**, 30, 421–426.
- [18] G. M. Sheldrick, *Acta Crystallogr., Sect. A* **1990**, 46, 467–473.
- [19] G. M. Sheldrick, University of Göttingen, Germany, **1997**.

Received December 10, 2003

Early View Article

Published Online May 5, 2004